

Study of Near-Electrode Plasma and Electrode Surface During Discharges in Electrolytes

D. L. Kirko*

National Research Nuclear University MEPhI, Moscow, 115409 Russia

*e-mail: dlkirko@mephi.ru

Received October 24, 2019; revised December 12, 2019; accepted December 19, 2019

Abstract—The cathode plasma of a discharge in an electrolyte based on sodium carbonate and sodium hydroxide is studied as well as its interaction with the surface of electrolytes made from tungsten, tantalum, and titanium. The electrotechnical properties of the discharge are measured by spectral methods and the electron temperature of the near-cathode plasma is determined. When tungsten electrodes are used, 0.2–1.5- μm -diameter thread-like structures appear on their surface. Interaction with the discharge current destroys tantalum electrodes. On the surface of titanium electrodes, 1–40- μm -diameter sphere-like formations and areas of a porous surface with a pore diameter of 0.1–1 μm are observed. The mechanism of the formation of these surface structures is discussed.

Keywords: discharge in electrolyte, plasma interaction with metal surface, sphere-like formations, thread-like structures

DOI: 10.1134/S1063780X20060045

1. INTRODUCTION

The ignition of the discharge in an electrolyte occurs when the current density increases near one of the electrodes, which causes the appearance of a glow near its surface [1–3]. In our experiments, the electrodes were either both immersed in the electrolyte, or one of them was placed near the surface of the electrolyte. The plasma region of the discharge in a liquid is surrounded by a steam–gas sheath, which is constantly in the state of intense boiling. In the pulse-periodic discharge regime, a breakdown phase is observed in the discharge, which is followed by an increase in the discharge current. Electric oscillations in the discharge circuit in a wide range of frequencies (30 kHz–200 MHz) were recorded [1, 4, 5]. The spectra of these oscillations were studied, and their possible cause, i.e., the appearance of plasma waves, is discussed.

We consider the practical applications of discharges in electrolytes, such as the surface modification of materials and polishing metal surfaces [1, 2, 6]. When the discharge is ignited above the electrolyte surface, it can be used in the systems of water and air purification [1, 7–10].

During the operation of plasma devices with high-current gas discharges, the formation of nanostructures was observed on the surface of electrodes made from graphite, pyrographite, and tungsten or on the walls of the chamber [11–13]. During discharges in electrolytes, micron-sized structures were discovered

on the surface of titanium electrodes [14]. In this work, we study the possibility of the appearance of micron structures on the surface of tungsten and tantalum electrodes depending on the characteristics of the near-electrode plasma.

2. ELECTROTECHNICAL CHARACTERISTICS OF THE DISCHARGE

In this work, we used cylindrical chambers with a volume of 200 to 350 cm^3 and a diameter of 8 to 14 cm made from plexiglass and electrolytes based on sodium carbonate (Na_2CO_3) and sodium hydroxide (NaOH). The experimental device is shown in Fig. 1. The cathodes were made in the shape of 1 to 2-mm-diameter rods made from tungsten (W), titanium (Ta), and tantalum (Ta) and the anodes were made from 0.2–0.4-mm-thick plates from stainless steel and molybdenum. The power source was a fullwave rectifier with a voltage of 0 to 240 V with a pulse repetition rate of 100 Hz. The cathode rod was placed vertically in a ceramic tube and submerged in the electrolyte at different depths relative to its surface. The working surface of the cathode was a small area of 0.5 to 1.5 mm^2 . In our experiments, the discharge was ignited inside the electrolyte and its ignition was accompanied by the appearance of a glow. The discharge image was recorded with a Nikon 1G serial photo camera with a time resolution of 1 ms according to its technical passport. This camera was placed at an

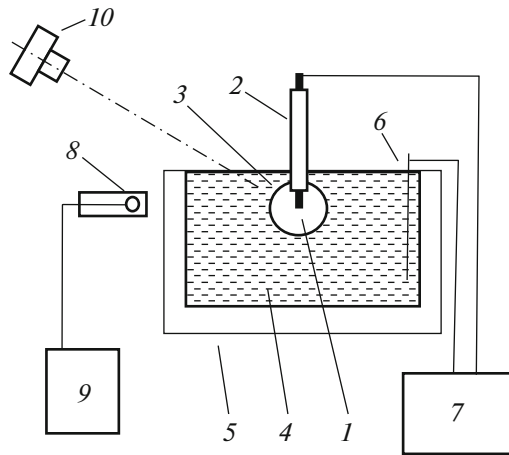


Fig. 1. Scheme of the experimental setup: (1) cathode, (2) ceramic tube, (3) discharge region, (4) electrolyte, (5) case, (6) anode, (7) power source, (8) magnetic probe, (9) spectrum analyzer, and (10) photo camera.

angle of 20° to 30° to the electrolyte's surface. To obtain higher quality images, we used a camera made from plexiglass with plexiglass windows. Figure 2a shows an image of the discharge with the cathode placed at ≈ 1.5 cm below the electrolyte's surface. This image was taken through the side window of the chamber. In these experiments, the dimensions of the glow region of the discharge were in the range 1.5–2.5 cm. The most intense radiation was recorded from the 3–5-mm-diameter near-cathode region, which is shown in Fig. 2b. The characteristic colors of the discharge, depending on the electrolyte's composition and concentration, are yellow–red and blue.

Let us consider the changes of the electrotechnical characteristics of the discharge in the electrolyte. The concentration of NaOH was chosen in the range $C = 0.4$ – 0.6 M. The concentration of Na_2CO_3 was $C = 1$ M, or 106 g per 10^3 cm^3 of distilled water. Figure 3 shows the current–voltage characteristic for a Ti cathode in a discharge in electrolyte based on Na_2CO_3 with a concentration $C = 0.5$ M. The effective values of cur-

rent I and voltage U are shown in the figure. The voltage was supplied to the electrodes through a fullwave rectifier (Fig. 4a).

Let us present the characteristic points of this dependence. The initial segment of the current–voltage characteristic is approximately linear. At point 1, at a voltage of 54 ± 2 V and current of 1.1 ± 0.1 A, the breakdown occurs and the discharge ignites near the cathode surface. The thickness of the cathode region is 1–2 mm. The ignition voltage depends on the concentration of the electrolyte [5]. On segment 1–2, when the current increases, the dimensions of the plasma region increase to 5–10 mm. At the same time, a steam–gas region is generated at the boundary between the plasma region and the electrolyte [5]. When the voltage and the power deposited in the discharge are increased, the resistance of the steam–gas region decreases. Segment 2–3 is close to linear and usually describes a stable regime of discharge operation. Therefore, the main measurements were conducted in this region of the current–voltage characteristic. After the maximum is reached, the discharge intensity decreases, and the discharge is quenched at point 4. The last 5–0 segment of the characteristic is usually also close to linear. The shape of the current–voltage characteristic in discharges for the W and Ta cathodes is the same as that in the discharge for the Ti cathode (Fig. 3) but has different discharge ignition voltages (point 1) and positions of points 2–5. In the previous works, we established the effect of the dependence of the electrolyte concentration on the shape of the current–voltage characteristic [15]. In general, the shape of the characteristic is similar to the hysteresis curve and depends on the concentration of the electrolyte in the solution. When the electrolyte concentration is decreased, the total area of the characteristic decreases, and when the concentration is increased, its area increases.

When a pulse repetition rate of 100 Hz is used, a breakdown and periodic ignition of a discharge in electrolyte occurs at this frequency (Fig. 4a). A single current pulse is a damped sinusoid with a period of

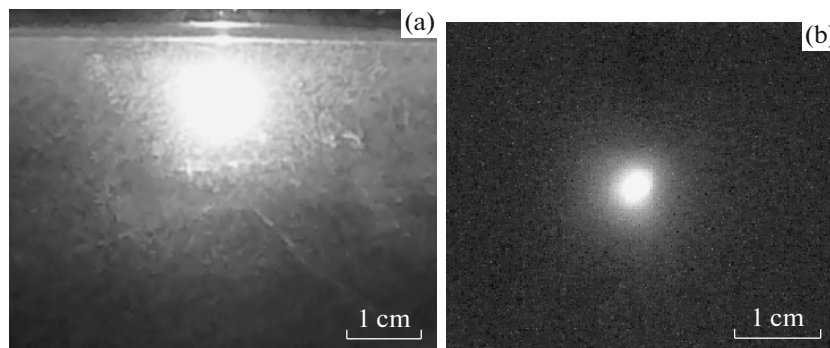


Fig. 2. Photograph of a discharge in electrolyte: (a) integral image of the discharge (exposition of 10 ms) and (b) image of the near-cathode region (exposition of 1 ms).

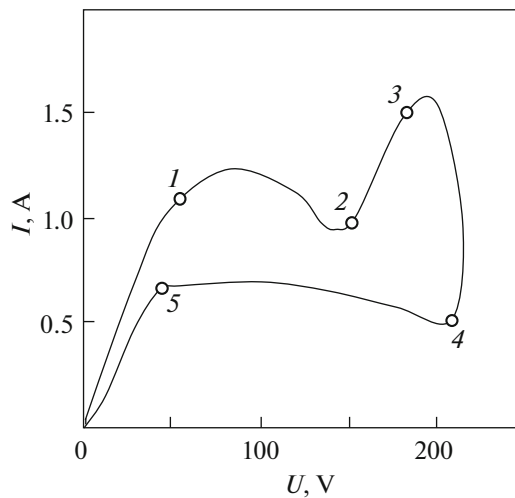


Fig. 3. Current–voltage characteristic of a discharge with a titanium cathode.

≈ 0.9 ms and the number of periods $n = 3-4$ (Fig. 4c). High-frequency oscillations are observed during the first period of the current. Earlier, we recorded electric oscillations of a discharge in an electrolyte in the following frequency ranges: 20–300 kHz and 5–80 MHz [5, 14, 15]. As a possible explanation, we considered the generation of ion cyclotron and electron cyclotron waves in the discharge plasma [16].

To describe the breakdown phase of the discharge in an electrolyte, we applied the model of the spark breakdown of a liquid containing gas bubbles [17]. According to this model, estimates were made of the ionization of the near-cathode medium, which contains hydrogen bubbles [14, 15].

3. SPECTRAL COMPOSITION OF THE RADIATION OF THE DISCHARGE IN AN ELECTROLYTE

To obtain a panoramic spectrum of the discharge radiation, we used an AvaSpec 2048 spectrometer with the wavelength range of 200 to 1000 nm and spectral resolution of 0.3 nm. The time dependence of the spectral lines was recorded using a MUM monochromator with a working spectral range of 200 to 800 nm and spectral resolution of 0.2 nm and a FEU-85 photomultiplier with a time resolution of 5 ns. The diagnostic system was calibrated using a SIRSH 8-200 lamp.

The radiation from the discharge in the electrolyte was focused on the entrance slit of the device using an achromatic condenser. The integral radiation from the entire discharge region was recorded. The maximum luminosity corresponds to the near-cathode discharge region. The electrolyte's transmittance was studied using the Specord M40 spectrophotometer. The transmittance coefficient of an electrolyte based on Na_2CO_3 ($C = 0.5$ M) in the wavelength range 300–

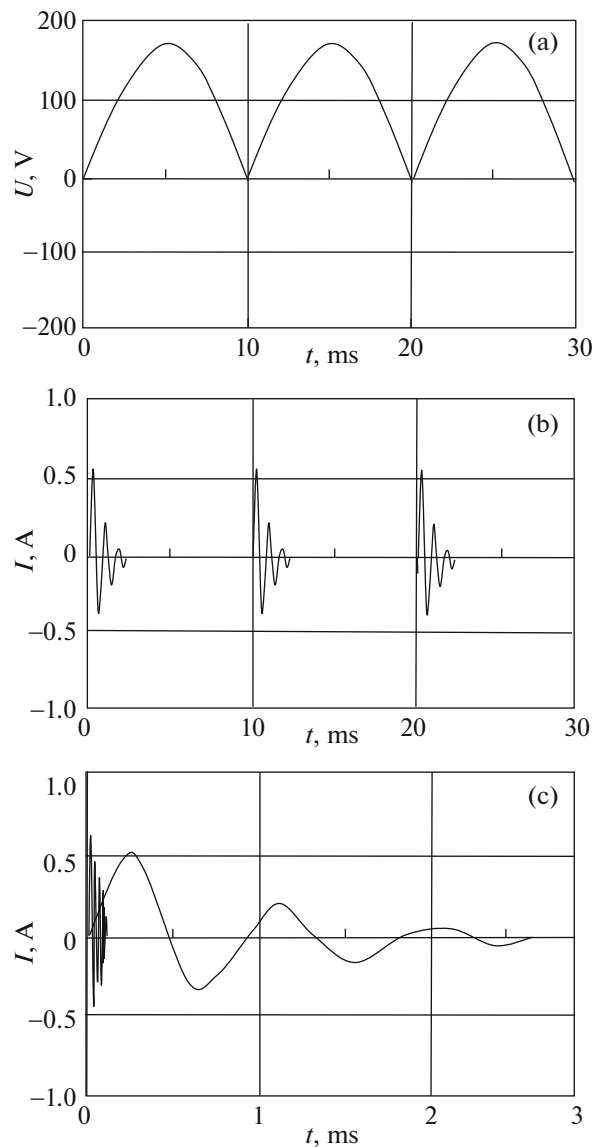


Fig. 4. Time dependences of voltage pulses on the discharge voltage (a) and the discharge current (b) in a discharge with a titanium cathode: synchronized variant and (c) single current pulse.

850 nm is in the range $k = 70-83\%$ for the solution's thickness of 1 cm. The intensities of the spectral lines were calculated taking into account the radiation absorption in the electrolyte.

In the experiments, regimes with different ratios of the spectral line intensities were studied depending on the discharge current in the linear 2–3 section of the current–voltage characteristic (Fig. 3). Figure 5 shows the radiation spectra of the discharge in an electrolyte for all three cathodes under study.

Let us consider the radiation spectrum of a discharge with a Ti cathode (Fig. 5a). The discharge was ignited in Na_2CO_3 ($C = 0.5$ M) in the working regime at current $I \approx 1.4$ A (2–3 section in Fig. 3). The maximum intensity in the spectrum is provided by the

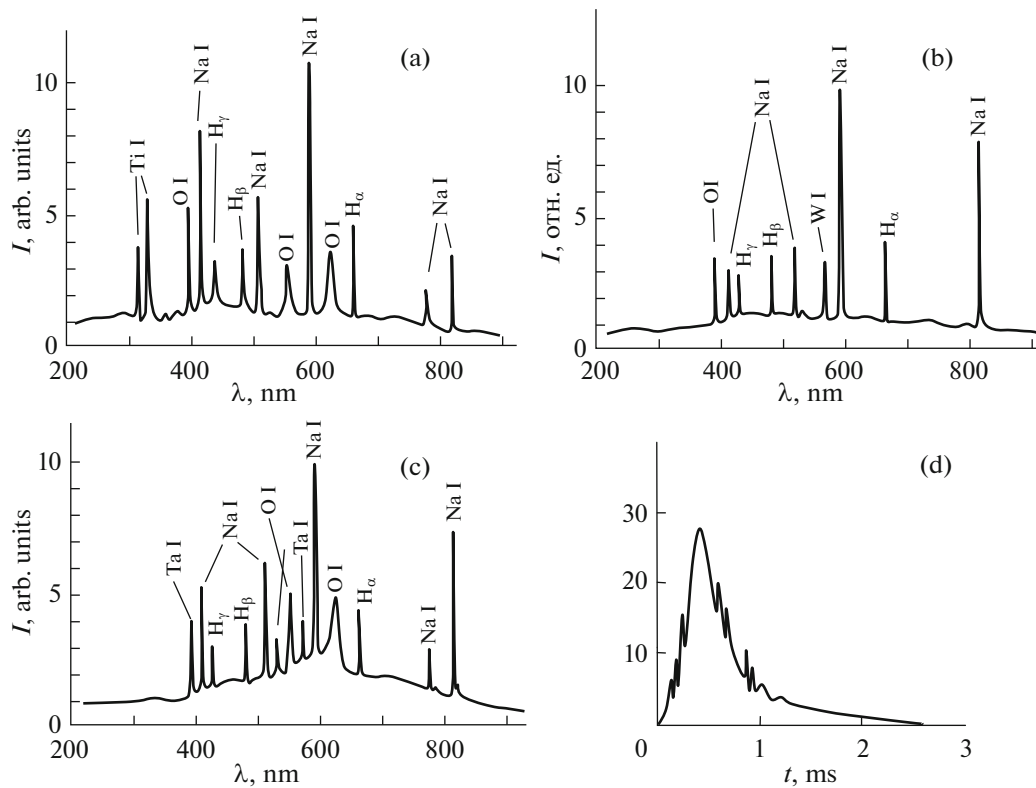


Fig. 5. Radiation spectrum of a discharge in an electrolyte depending on the cathode material: (a) titanium cathode, (b) tungsten cathode, and (c) tantalum cathode. (d) Time dependence of the sodium atomic line Na I 589 nm in a discharge with a titanium cathode. The discharge current in all experiments was $I \approx 1.4$ A.

atomic sodium lines Na I 589 and 424 nm. The minimum intensity is observed for the following lines: atomic titanium Ti I 337 and 323 nm; atomic sodium Na I 515, 819, and 781 nm; atomic hydrogen H_α 656 nm, H_β 486 nm, and H_γ 434 nm; and atomic oxygen O I 395.5, 555, and 627 nm. In this discharge operation regime, we made the assumption that the plasma state can be described by the model of the local thermal equilibrium [18]. Therefore, we calculated the electron plasma temperature in the near-cathode region by the method of relative intensities, using the atomic hydrogen lines H_α and H_β . This temperature was $T = 2800 \pm 200$ K (the current $I = 1.4$ A).

In the spectrum of the discharge with a W cathode (Fig. 5b) at current $I \approx 1.4$ A in the 2–3 section of the current–voltage characteristic (Fig. 3) ignited in Na_2CO_3 ($C = 0.5$ M), the lines with maximum intensity are Na I 589 and 819 nm. The minimum intensity lines are Na I 424 and 519 nm, W I 569 nm, O I 395.5 nm, H_α 656 nm, H_β 486 nm, and H_γ 434 nm. In this regime, we also assume that the local thermal equilibrium was achieved [18]. The electron plasma temperature in the near-cathode region determined by the relative intensities' method using the atomic hydrogen lines H_α and H_γ is $T = 3100 \pm 200$ K (the current $I = 1.4$ A).

The spectrum of the discharge in Na_2CO_3 ($C = 0.5$ M) with a Ta cathode was recorded at the same

current $I \approx 1.4$ A in the 2–3 section of the current–voltage characteristic. A characteristic feature of this spectrum is the presence of a continuous component in the range 400–900 nm (Fig. 5c). The lines with maximum intensity in the spectrum are Na I 589 and 819 nm. The lines with minimum intensity are Na I 424, 519, and 781 nm; O I 555 and 627 nm; H_α 656 nm; H_β 486 nm; H_γ 434 nm; and Ta I 397, 546, and 566 nm. It was assumed that the plasma's state can be described by the local thermal equilibrium model in this case as well [18]. The electron temperature determined by the relative intensities' method using the H_α and H_β lines is $T = 3200 \pm 200$ K (the current $I = 1.4$ A).

The characteristic time dependence of the atomic sodium line Na I 589 nm in the experiment with the Ti cathode is shown in Fig. 5d. Oscillation processes with frequencies 11.5 ± 0.3 kHz and 14.2 ± 0.3 kHz were observed in the radiation profile of this line. Earlier, oscillations with frequencies ≈ 5.9 and ≈ 5.3 kHz were observed in the profiles of the H and W lines [5].

4. STUDY OF THE ELECTRODE SURFACE AFTER INTERACTION WITH THE DISCHARGE

We conducted experiments on the interaction between the discharge in an electrolyte and the surface of W, Ti, and Ta electrodes. The duration of these

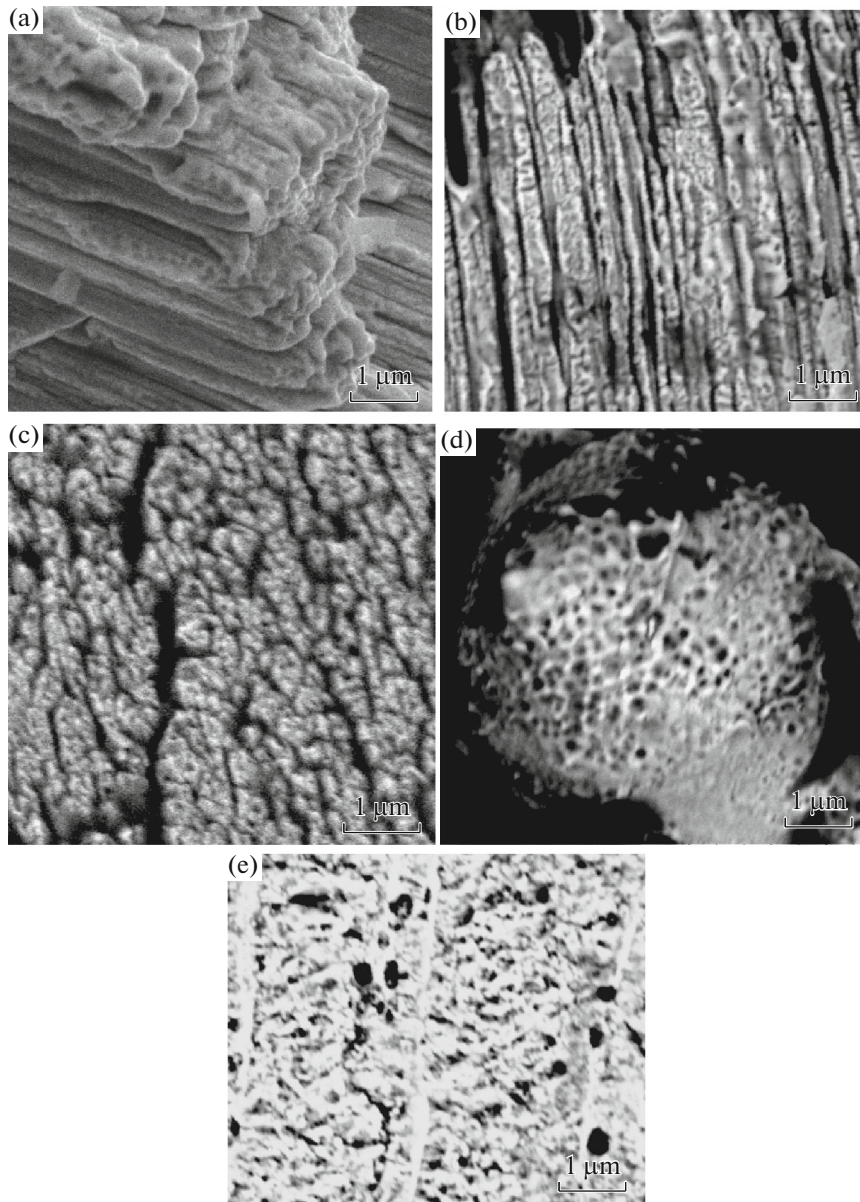


Fig. 6. SEM images of the W cathode surface after exposure to a discharge in electrolyte: (a) cathode end, (b) thread-like structures, (c) cellular structures, (d) sphere-like objects, and (e) electrode surface before exposure to the discharge.

experiments was chosen in the range 5–60 min. The area of the cathode surface through which the discharge current passed was 0.5–1.5 mm². The current density was in the range 0.2–3 A/mm². The temperature of the near-anode region determined by spectral measurements was 2800–3200 K. These values are higher than the melting temperatures of Ti ($t_{Ti} \approx 1608^\circ\text{C}$) and Ta ($t_{Ta} \approx 2996^\circ\text{C}$) but lower than the melting temperature of W ($t_W \approx 3420^\circ\text{C}$).

In these experiments, the discharge was switched on at the given time in the working regime of the current–voltage characteristic (segment 2–3 in Fig. 3) and the changes of the structure of the electrode sur-

face were studied after processing with the discharge using the VEGA 3 and Hitachi TM1000 scanning electron microscopes (SEM).

In the case of the W cathode, the initial 1-mm-diameter W wire had a fibrous texture. This was determined by cutting the wire with snip cutters, which produced 0.1–0.2-mm long cracks along the wire and very thin 0.1–0.3-mm-long splinters of irregular shape. The sheeting of W is also manifested at the microscopic level. (The SEM image of the surface of W electrodes before interaction with the discharge will be discussed later.) Figure 6a shows the region near the cathode end after interaction with the discharge in the

electrolyte. The layered structure of W is seen, as well as the 0.1–1.5- μm -diameter filaments. The length of the filaments is 100–200 μm . The ends of some filaments are thickened and resemble fire-polishing.

After the discharge, deep 50–250- μm -long and 5–10- μm -wide cracks appeared on the W surface. A detailed study of the surface near the cracks revealed regions that contain 0.1–1.2- μm -diameter filaments (Fig. 6b). Apparently, they appear under the action of the discharge. We can assume that filamentation of the current occurs during the discharge in an electrolyte and the filaments have a diameter of 0.1 to 1 μm . This phenomenon requires further investigation. At the same time, areas with cellular structures with a cell size of 0.2 to 1.0 μm are also present at the end of the W cathode (Fig. 6c). This granulation shape is frequently observed in the rapid cooling of the metal melts [19]. Another interesting type of objects found on the surface of the W electrode are 2–15- μm -diameter sphere-like formations (Fig. 6d) with a porous surface (pore size 0.2–1.0 μm). Some of these formations have an irregular shape and small flakes of metal on their surface.

An image of a W electrode surface before interaction with the discharge is shown in Fig 6d. On this surface, 1–4- μm -size irregular holes were found.

At the surface of Ti electrodes, 1–40- μm -diameter sphere-like formations are observed. At the same time, blobs of irregular shape are found near the spheres, as well as a dense population of small sphere-like irregular-shaped formations of 0.1 to 2.0 μm . It is possible that these small formations are seeds for the formation of larger sphere-like structures. Also, 0.2–1.0- μm -wide cracks are observed on the surface.

Energy-dispersive analysis of the element composition of this surface revealed the percentage of the composition of its elements: O 71%, Ti 25%, and Na 4% (the determination error was $\pm 2\%$). For this analysis, we used a unit built into the VEGA 3 SEM microscope. The initial cathode material, before submersion in an electrolyte and exposure to the discharge, contains 98% of Ti (with an error of $\pm 2\%$). Compared to the content of the electrode material Ti, the oxygen content after exposure is quite high. Na is contained in the electrolyte in the form of ions and can penetrate into the surface in significant quantities. Analysis of the composition of the sphere-like formations gave the following values: O 71% and Ti 29% (with an error of $\pm 2\%$). A Ti IV compound that contains large quantities of O could be Ti hydroxide $\text{TiO}_2 \cdot n\text{H}_2\text{O}$ ($\text{TiO}_2 \cdot 2\text{H}_2\text{O}$ or $\text{Ti}(\text{OH})_4$). In this case, the oxygen content on the surface can quadruple. Our microscopes, unfortunately, do not distinguish oxygen. Near the surface of the cathode, the electrolysis of water accompanied by oxygen release can also occur. Therefore, another possible Ti compound is titanium dioxide, TiO_2 . The depth of the surface layer on which the content of the elements is analyzed is determined by the penetration

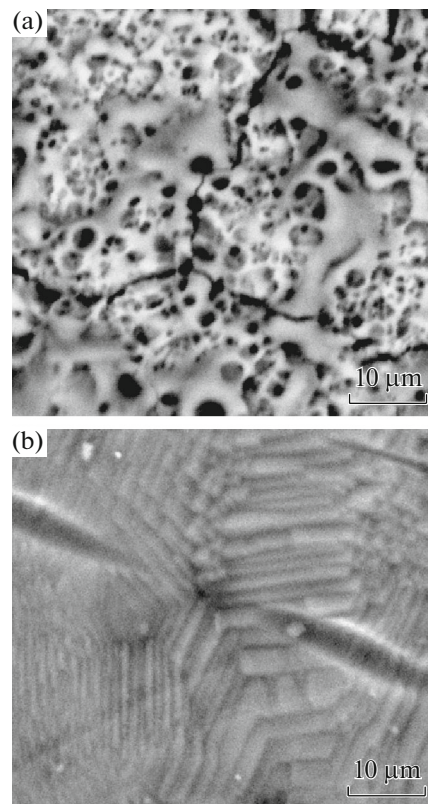


Fig. 7. SEM images of a titanium cathode after exposure to a discharge in electrolyte: (a) porous surface, and (b) electrode surface before exposure to the discharge.

depth of the scanning electron beam of the VEGA 3 SEM microscope and it is 3.5–4.2 μm .

A porous surface is another surface structure that develops on the Ti cathode (Fig. 7a). Irregular pores of 0.1 to 1 μm are found on the electrode surface. The typical shape of the pores is oval. Clusters of small pores of 0.1 to 0.3 μm are observed. Cracks with an irregular shape and a size of 0.2 to 0.5 μm are also found on the surface. The surface of the Ti electrode after exposure to the discharge is shown in Fig. 7b. This surface is characterized by ribbed structures with a period in the range 1–3 μm and technological grooves obtained during the manufacture of Ti wire.

Taking into account the presence of a porous structure on the surface of the Ti electrode, let us consider the properties of the electric current near this electrode. We can assume that, near the electrode, the discharge current is filamented into multiple separate 0.1–2- μm -diameter current channels with the current of 10^{-8} to 10^{-6} A flowing through each channel.

On the surface of Ta cathodes after exposure to the discharge, deep 10–100- μm -wide and 100–500- μm -long cracks are observed, as well as the appearance of 1–5- μm -size microdips. After lengthy exposure to the discharge (50–60 min), the size of the cracks

increases, and the flaking of small 100–400- μm surface bits is observed. The effects under study lead to the intense destruction of the surface of Ta electrodes.

Below, we give recommendations for the use of W, Ti, and Ta cathodes in experiments on discharges in an electrolyte. The initial shape of the cathode in these experiments is conical and it is later deformed and destroyed under the action of the discharge. Using Ta cathodes is undesirable due to their strong destruction in the described regime of the discharge in an electrolyte.

Using W wire requires a high-quality processing of the cathode end, which is difficult because of the fragility and sheeting of W. At the same time, W cathodes have the greatest longevity and they keep their initial shape the longest during the interaction with the discharge.

Using Ti wire as a cathode, we can obtain the desired shape of the cathode end. Since the Ti melting temperature is lower, the end of the Ti cathodes is destroyed faster compared to W cathodes, meaning that larger diameter cathodes are required. For cathodes from W and Ti, we should also check the structure of the surface of the material and ensure that it is free from microcracks and microholes.

5. CONCLUSIONS

In this work, we have studied the near-electrode plasma of a discharge in electrolyte and the interaction of the discharge plasma with the surface of the electrodes. The dependence of the characteristics of the discharge on the material of cathodes made from W, Ti, and Ta was studied. Spectral measurements were used to determine the electron's temperature of the discharge in the near-cathode region, which, for the cathodes under study, was in the range $T = 2800\text{--}3200\text{ K}$.

For W cathodes, thread-like structures 0.1–1.5 μm in diameter and 100–200 μm long are observed on their surface. At the same time, in some areas, the surface is granulated with cells of 0.2 to 1.0 μm , and sphere-like objects 2–15 μm in diameter with a microporous surface are also observed. The growth of the discovered structures on the surface of the W cathode, apparently, occurs due to the filamentation of the discharge current and interaction of the resulting microcurrents with the metal surface.

In the case of Ta cathodes, 10–100- μm -wide cracks and microdips are observed on the surface, which lead to its destruction.

On the surface of Ti cathodes, sphere-like formations with a diameter of 0.5 to 40 μm and areas of a porous surface with pores of 0.1 to 1 μm are observed. Element analysis of the surface of the Ti electrode and the sphere-like formations showed that Ti IV hydroxide is present in both. The discovery of small sphere-

like germs 0.5–1 μm in diameter on the surface demonstrates that such formations grow. A possible reason for such growth is the minimization of the surface cohesive energy of Ti IV hydroxide molecules characteristic of sphere-like surfaces.

REFERENCES

1. Al. F. Gaisin, N. F. Kashapov, A. I. Kuputdinova, and R. A. Mukhametov, *Tech. Phys.* **63**, 695 (2018).
2. R. R. Kayumov, Al. F. Gaisin, E. E. Son, Az. F. Gaysin, and F. M. Gaysin, *Phys. Scr.* **2010** (T142), 014038 (2010).
3. F. M. Gaisin and E. E. Son, *Electrophysical Processes in Discharges with Solid and Liquid Electrodes* (Izd. Ural'skogo Univ., Sverdlovsk, 1989) [in Russian].
4. F. M. Kanarev, *Low Current Electrolysis of Water* (Izdvo Krasnodarskogo Univ., Krasnodar, 2010) [in Russian].
5. D. L. Kirko, *Tech. Phys.* **60**, 505 (2015).
6. I. V. Suminov and A. V. Epel'fel'd, *Pribory*, No. 9, 13 (2001).
7. S. Samukawa, M. Hori, S. Rauf, K. Tachibana, P. Bruggeman, G. Kroesen, J. C. Whitehead, A. B. Murphy, A. F. Gutsol, S. Starikovskaia, U. Kortshagen, J.-P. Boeuf, T. J. Sommerer, M. J. Kushner, U. Czarnetzki, et al., *J. Phys. D: Appl. Phys.* **45**, 253001 (2012).
8. P. Bruggeman and Ch. Leys, *J. Phys. D: Appl. Phys.* **42**, 053001 (2009).
9. V. V. Rybkin and D. A. Shutov, *Plasma Phys. Rep.* **43**, 1089 (2017).
10. B. Pongrac and Z. Machala, *IEEE Trans. Plasma Sci.* **39**, 2664 (2011).
11. V. I. Krauz, Yu. V. Martynenko, N. Yu. Svechnikov, V. P. Smirnov, V. G. Stankevich, and L. N. Khimchenko, *Phys.—Usp.* **53**, 1015 (2010).
12. V. I. Krauz, L. N. Khimchenko, V. V. Myalton, V. P. Vinogradov, Yu. V. Vinogradova, V. M. Gureev, V. S. Koidan, V. P. Smirnov, and V. E. Fortov, *Plasma Phys. Rep.* **39**, 289 (2013).
13. B. M. Smirnov, *Phys.—Usp.* **60**, 1236 (2017).
14. D. L. Kirko and A. S. Savjolov, *J. Phys.: Conf. Ser.* **941**, 012018 (2017).
15. D. L. Kirko and A. S. Savjolov, *J. Phys.: Conf. Ser.* **747**, 012002 (2016).
16. N. A. Krall and A. W. Trivelpiece, *Principles of Plasma Physics* (Academic, New York, 1973).
17. S. M. Korobeinikov, A. V. Melekhov, and A. S. Besov, *High Temp.* **40**, 652 (2002).
18. *Plasma Diagnostic Techniques*, Ed. by R. H. Huddlestone and S. L. Leonard (Academic, New York, 1965).
19. A. M. Glezer and I. E. Permyakova, *Nanocrystals Hardened from Melt* (Fizmatlit, Moscow, 2012) [in Russian].
20. G. Cao and Y. Wang, *Nanostructures and Nanomaterials. Synthesis, Properties, and Applications*, 2nd ed. (World Scientific, Singapore, 2010).

Translated by E. Voronova